

Prethermalization and thermalization in models with weak integrability breaking

Bruno Bertini,¹ Fabian H.L. Essler,¹ Stefan Groha,¹ and Neil J. Robinson^{1,2}

¹*The Rudolf Peierls Centre for Theoretical Physics,
University of Oxford, Oxford, OX1 3NP, United Kingdom*

²*Condensed Matter Physics and Materials Science Department,
Brookhaven National Laboratory, Upton, New York 11973, USA*

(Dated: October 19, 2015)

We study the effects of integrability breaking perturbations on the non-equilibrium evolution of many-particle quantum systems. We focus on a class of spinless fermion models with weak interactions. We employ equation of motion techniques that can be viewed as generalizations of quantum Boltzmann equations. We benchmark our method against time dependent density matrix renormalization group computations and find it to be very accurate as long as interactions are weak. For small integrability breaking, we observe robust prethermalization plateaux for local observables on all accessible time scales. Increasing the strength of the integrability breaking term induces a “drift” away from the prethermalization plateaux towards thermal behaviour. We identify a time scale characterizing this cross-over.

In classical mechanics, integrable few-particle systems can be understood in terms of periodic, non-ergodic motion in action-angle variables. Breaking integrability by adding a weak perturbation induces a fascinating crossover between integrable and chaotic motion, which is described by the celebrated KAM theory [1]. In essence, classical few-particle systems with weak integrability breaking retain aspects of integrable motion on intermediate time scales. Recently it has emerged, that similar behaviour occurs in the non-equilibrium evolution of isolated many-particle quantum systems. Starting with the seminal work of Rigol et al [2] it has become clear that there is a dramatic difference between the late time behaviour of isolated integrable and non-integrable quantum many particle systems prepared in initial states that are not eigenstates of the Hamiltonian. Generic systems *thermalize* [2–13], i.e. exhibit relaxation of local observables towards a Gibbs ensemble with an effective temperature, while integrable systems evolve towards a generalized Gibbs ensemble [2, 12–35]. Starting with the work of Moeckel and Kehrein [36] it was then realized that models with weak integrability breaking perturbations exhibit transient behaviour, in which local observables relax towards non-thermal values that retain information of the proximate integrable theory. This has been termed *prethermalization*, and has been established to occur in several models [36–46]. Crucially, it was recently observed in experiments on ultra-cold bosonic atoms [47–49]. The general expectation is that prethermalization is a transient effect, and at “sufficiently late times” non-integrable systems thermalize. While this appears natural, there is scant evidence in support of this scenario. The reason is that available numerical [50] or analytical [36, 41, 45] methods are not able to reach late enough times. The exception is the case of infinitely many dimensions, where it was shown in a particular example that a weakly non-integrable model thermalizes [51]. Here we address these issues in the context of weakly interacting

one dimensional many-particle systems. This case has the important advantage that the accuracy of approximate methods can be benchmarked by comparisons with powerful numerical methods like the time dependent density matrix renormalization group (t-DMRG) [50]. Moreover, the existence of many strongly interacting one dimensional integrable systems makes it possible to verify that the qualitative behaviour we find persists for arbitrary interaction strengths.

We focus on the weak interaction regime $U \lesssim J_1$ of the three-parameter family of spinless fermion Hamiltonians

$$H(J_2, \delta, U) = -J_1 \sum_{l=1}^L \left[1 + (-1)^l \delta \right] \left(c_l^\dagger c_{l+1} + \text{H.c.} \right) - J_2 \sum_{l=1}^L \left[c_l^\dagger c_{l+2} + \text{H.c.} \right] + U \sum_{l=1}^L n_l n_{l+1}. \quad (1)$$

Here c_i and c_i^\dagger are spinless fermion operators on site i and the hopping amplitudes describe nearest-neighbor and next-nearest-neighbor hopping respectively, while $0 \leq \delta < 1$ is a dimerization parameter. Finally there is a repulsive nearest neighbour interaction of strength U . From here onwards we set $J_1 = 1$ and measure all the energies in units of J_1 . There are several limits in which (1) becomes integrable: (i) $U = 0$ describes a free theory; (ii) $\delta = J_2 = 0$ corresponds to the anisotropic spin-1/2 Heisenberg chain [52]; (iii) the low-energy degrees of freedom for $J_2 = 0$ and $\delta, U \ll 1$ are described by the quantum sine-Gordon model [53]. Away from these limits, the model is non-integrable. Our protocol for inducing and analyzing non-equilibrium dynamics is as follows. We prepare the system in an initial density matrix ρ_0 that is not an eigenstate of $H(J_2, \delta, U)$ for any value of U . We then compare the expectation values of local operators for time evolution with the integrable $H(J_2, \delta, 0)$ and (weakly) non-integrable $H(J_2, \delta, U)$ respectively. For $U = 0$ our model is non-interacting, and concomitantly in the thermodynamic limit expectation

values of local operators relax to time independent values described by a generalized Gibbs ensemble. In the following we analyze how a small integrability breaking interaction $U > 0$ changes the non-equilibrium evolution. We stress that our protocol differs in a very important way from the weak interaction quenches analyzed previously [51, 54]. In these works there is no dynamics at all for $U = 0$. Hence quenching the interaction from zero to a finite value simultaneously breaks integrability and induces a time dependence into the problem. This masks the interaction induced modification of the integrable post-quench dynamics. Quantum quenches in the model (1) with $J_2 = 0$ were previously studied in Ref. [41] by numerical and analytical methods. On the accessible time scales robust prethermalization was observed, but no evidence for eventual thermalization was found. While our manuscript was being completed a paper appeared in which techniques similar to the ones we employ here were used to analyze quantum quenches in the case $\delta_i = \delta_f = 0$ [54]. No prethermalization in our sense was observed for the aforementioned reason that there is no dynamics without integrability breaking in this case, but instead evolution towards a thermal steady state was found. Given that U is small, a convenient basis for ana-

lyzing quench dynamics is obtained by diagonalizing the quadratic part of the Hamiltonian. This results in

$$H(J_2, \delta, 0) = \sum_{\alpha=\pm} \sum_{k>0} \epsilon_{\alpha}(k) a_{\alpha}^{\dagger}(k) a_{\alpha}(k), \quad (2)$$

where $a_{\pm}(k)$ are momentum space annihilation operators obeying canonical anticommutation relations $\{a_{\alpha}(k), a_{\beta}^{\dagger}(q)\} = \delta_{\alpha,\beta} \delta_{k,q}$, and $\epsilon_{\alpha}(k) = -2J_2 \cos(2k) + 2\alpha \sqrt{\delta^2 + (1 - \delta^2) \cos^2(k)}$ are single particle dispersion relations of the two bands of fermions. The system is initially (at time $t = 0$) prepared in a density matrix ρ_0 , and subsequently evolves according to

$$\rho(t) = e^{-iH(J_2, \delta_f, U)t} \rho_0 e^{iH(J_2, \delta_f, U)t}. \quad (3)$$

Using equation of motion (EOM) techniques [51, 55] analogous to the ones employed in derivations of quantum Boltzmann equations [56, 57], we obtain evolution equations for the two-point functions

$$n_{\alpha\beta}(q, t) = \text{Tr}[\rho(t) a_{\alpha}^{\dagger}(q) a_{\beta}(q)]. \quad (4)$$

The EOM can be cast in the form

$$\begin{aligned} \dot{n}_{\alpha\beta}(k, t) &= i\epsilon_{\alpha\beta}(k) n_{\alpha\beta}(k, t) + 4iU e^{it\epsilon_{\alpha\beta}(k)} \sum_{\gamma_1} J_{\gamma_1\alpha}(k; t) n_{\gamma_1\beta}(k, 0) - J_{\beta\gamma_1}(k; t) n_{\alpha\gamma_1}(k, 0) \\ &\quad - U^2 \int_0^t dt' \sum_{\gamma} \sum_{k_1, k_2 > 0} K_{\alpha\beta}^{\gamma}(k_1, k_2; k; t - t') n_{\gamma_1\gamma_2}(k_1, t') n_{\gamma_3\gamma_4}(k_2, t') \\ &\quad - U^2 \int_0^t dt' \sum_{\underline{\gamma}} \sum_{k_1, k_2, k_3 > 0} L_{\alpha\beta}^{\underline{\gamma}}(k_1, k_2, k_3; k; t - t') n_{\gamma_1\gamma_2}(k_1, t') n_{\gamma_3\gamma_4}(k_2, t') n_{\gamma_5\gamma_6}(k_3, t'), \end{aligned} \quad (5)$$

where $\epsilon_{\alpha\beta}(k) = \epsilon_{\alpha}(k) - \epsilon_{\beta}(k)$. Explicit expressions for the kernels J , K , L and details of our derivation are given in the Supplemental Material. The solution of the set of integro-differential equations (5) is numerically demanding. We designed an algorithm that scales as $L^3 \times T$ where T is the number of time steps and L the number of lattice sites. This allows us to reach long times $J_1 t \sim 80$ on large systems $L \sim 320$ (a similar scaling was proposed in Ref. [54]). Given the expectation values (4), we may readily calculate the single-particle Green's function

$$\begin{aligned} \mathcal{G}(j, l; t) &= \text{Tr}[\rho(t) c_j^{\dagger} c_l] \\ &= \frac{1}{L} \sum_{k>0} \sum_{\alpha, \beta = \pm} \gamma_{\alpha}^*(k, j) \gamma_{\beta}(k, l) n_{\alpha\beta}(k, t), \end{aligned} \quad (6)$$

where the coefficients $\gamma_{\alpha}(k, j)$ are given in the Supplemental Material. A crucial check of the accuracy of our approach is provided by a direct comparison to previous t-DMRG computations [41]. In Fig. 1 we present

a comparison of $\mathcal{G}(L/2, L/2 + 1)$ between EOM and t-DMRG results for a quench where the system is prepared in the ground state of $H(0, 0.8, 0)$ and time evolved subject to the Hamiltonian $H(0, 0.4, 0.4)$. We see that even for relatively large $U = 0.4$, there is excellent agreement between the two methods for all times accessible by t-DMRG. Similar levels of agreement are found for other $\mathcal{G}(L/2, L/2 + j)$ with $j = 2, 3, 4, 5$. This agreement suggests that the EOM method is very accurate for small values of U and short and intermediate time scales. The advantage of the EOM method is that it allows us to access later time scales than the t-DMRG computations reported in Ref. [41]. As long as the interaction strength U is sufficiently small, we observe very long-lived prethermalization plateaux, as is exemplified in the inset in Fig. 1. There, the thermal value has been computed by quantum Monte Carlo simulations on a system with $L = 100$ sites.

In order to investigate if and how the prethermalized

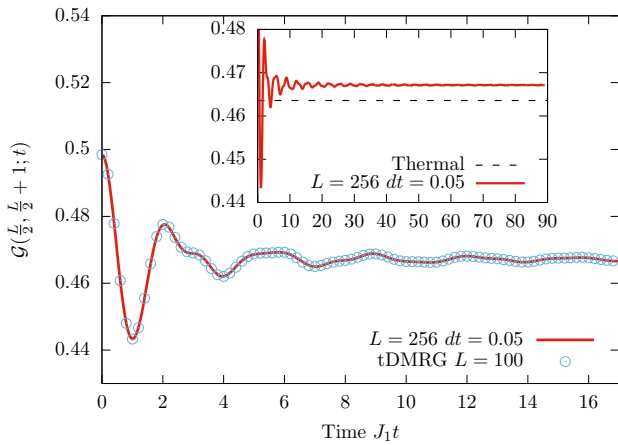


FIG. 1. (Color online) $\mathcal{G}(\frac{L}{2}, \frac{L}{2} + 1; t)$ for a quench where the system is prepared in the ground state of $H(0, 0.8, 0)$ and time evolved with $H(0, 0.4, 0.4)$ for a system with $L = 256$ sites. The EOM results (red line) are in excellent agreement with t-DMRG computations [41] (circles). Inset: prethermalized behaviour persists over a large time interval.

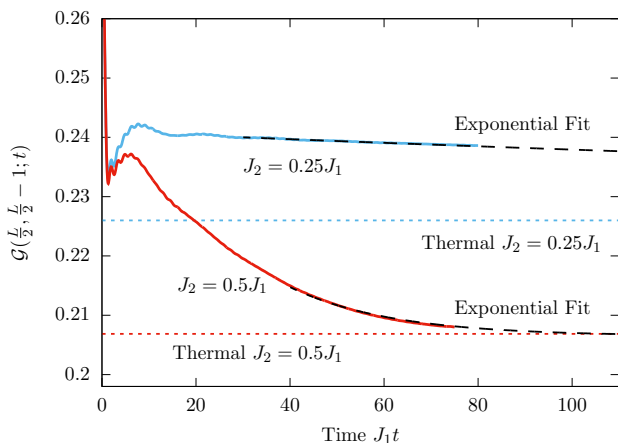


FIG. 2. (Color online) $\mathcal{G}(\frac{L}{2}, \frac{L}{2} - 1; t)$ for a system with Hamiltonian $H(J_2, 0.1, 0.4)$ and sizes $L = 360, 320$ initially prepared in a thermal state (7) with density matrix $\rho(2, 0, 0, 0)$. The expected steady state thermal values are indicated by dotted lines, while the black dashed lines are exponential fits to (8).

regime evolves towards thermal equilibrium it is convenient to invoke a non-zero J_2 . In essence, J_2 allows us to tune the cross-over time scale between the two regimes. In order to access the dynamics for a larger range of energy densities we consider thermal initial density matrices of the form

$$\rho(\beta, J_2, \delta, U) = \frac{e^{-\beta H(J_2, \delta, U)}}{\text{Tr}(e^{-\beta H(J_2, \delta, U)})}. \quad (7)$$

Figs. 2 and 3 show results for the time evolution of the Green's function for a system prepared in the initial state (7) with density matrix $\rho(2, 0, 0, 0)$, and time evolved with Hamiltonian $H(J_2, 0.1, 0.4)$. In contrast to

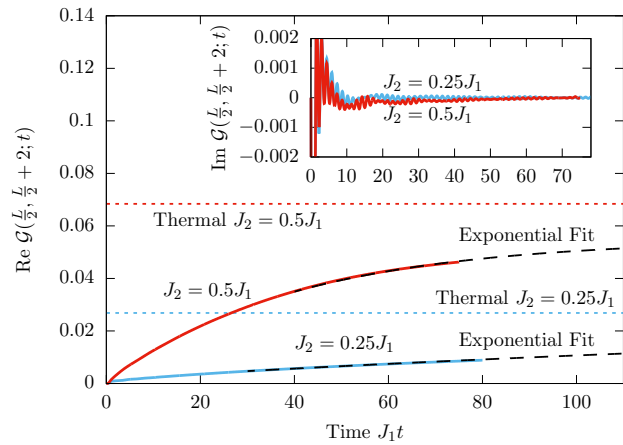


FIG. 3. (Color online) Real (Inset: imaginary) part of $\mathcal{G}(\frac{L}{2}, \frac{L}{2} + 2; t)$ for a system with Hamiltonian $H(J_2, 0.1, 0.4)$ and sizes $L = 360, 320$, that was initially prepared in a thermal state (7) with density matrix $\rho(2, 0, 0, 0)$. The expected steady state thermal values are indicated by dotted lines, while the black dashed lines are exponential fits to (8).

the case $J_2 = 0, U = 0.4$, we now observe a slow drift towards a thermal steady state. Increasing J_2 enhances the drift. The thermal values shown in Figs. 2 and 3 are obtained as follows. The energy density is given by $e = \text{Tr}[\rho(2, 0, 0, 0)H(J_2, 0.1, 0.4)]/L$ and determines the effective temperature $1/\beta_{\text{eff}}$ of the thermal ensemble for the post-quench Hamiltonian $H(J_2, 0.1, 0.4)$ through $e = \text{Tr}[\rho(\beta_{\text{eff}}, J_2, 0.1, 0.4)H(J_2, 0.1, 0.4)]/L$ [58]. We determine β_{eff} by exact diagonalization of small systems up to size $L = 16$, and then use the same method to compute the single-particle Green's function in thermal equilibrium at temperature $1/\beta_{\text{eff}}$. We note that $\mathcal{G}(i, j; t)$ is real for odd separations $|i - j|$. For even $|i - j|$ the imaginary part is non-zero but small and relaxes towards zero. We find that the observed relaxation towards thermal values is compatible with exponential decay

$$\mathcal{G}(i, j; t) \sim \mathcal{G}(i, j)_{\text{th}} + A_{ij}(J_2, \delta, U)e^{-t/\tau_{ij}(J_2, \delta, U)}, \quad (8)$$

where $\mathcal{G}(i, j)_{\text{th}}$ is the thermal Green's function at temperature $1/\beta_{\text{eff}}$ [59]. The decay times $\tau_{ij}(J_2, \delta, U)$ are quite sensitive to the value of J_2 . This can be understood by noting that large values of J_2 modify the band structure of the non-interacting model by introducing additional crossings at a fixed energy. This, in turn, generates additional scattering channels that promote relaxation.

A natural question is whether the integral equation (5) can be simplified in the late time regime by removing the time integration, in analogy with standard quantum Boltzmann equations (QBE) [56, 57]. Here we are faced with the difficulty that the structure of our EOM (5) is quite different from the ones studied in Refs [56, 57]. However, in the case $\delta_f = 0$ numerical integration of the full EOM (5) suggests that the ‘‘off-diagonal’’ occupation

numbers become negligible at late times $n_{+-}(k, t) \approx 0$ and it is possible to derive a QBE for “diagonal” occupation numbers. The QBE for $\delta_f = 0$ reads

$$\begin{aligned} \dot{n}_{\alpha\alpha}(k, \tau) = & - \sum_{\gamma, \delta} \sum_{p, q > 0} \tilde{K}_{\alpha\alpha}^{\gamma\delta}(p, q; k) n_{\gamma\gamma}(p, \tau) n_{\delta\delta}(q, \tau) \\ & - \sum_{\gamma, \delta, \epsilon} \sum_{p, q, r > 0} \tilde{L}_{\alpha\alpha}^{\gamma\delta\epsilon}(p, q, r; k) n_{\gamma\gamma}(p, \tau) n_{\delta\delta}(q, \tau) n_{\epsilon\epsilon}(r, \tau). \end{aligned} \quad (9)$$

Here $\tau = U^2 t$ is the usual rescaled time variable, $t_0 \gg 1/U$ is the time at which the kinetic equation is initialized and the functions \tilde{K} , \tilde{L} are given in the Supplemental Material. The QBE agrees with the EOM for sufficiently late times (an example is shown in Fig. 4, see the discussion below). Because of its simpler structure, the QBE allows us to access later times than we are able to reach with the EOM approach. In particular, employing the QBE we conclude that for weak interactions the relaxation times in (8) scale as [60]

$$\tau_{ij}^{-1}(J_2, \delta_f = 0, U) \propto U^2. \quad (10)$$

This is in contrast to the U^4 scaling found for interaction quenches in the infinite dimensional Hubbard model [51].

To establish more comprehensively that the integrability breaking perturbation leads to thermalization, we consider the (Bogoliubov) mode occupation numbers $n_{\alpha\beta}(q, t)$ themselves. The mode occupation operators are not local in space, and hence it is not a priori clear that their expectation values should eventually thermalize; see however Ref. [61]. Importantly, we only consider initial states with finite correlation lengths, which implies that $\mathcal{G}(j, l; t)$ are exponentially small in $|j - l|$ as long as $|j - l| \gg J_1 t$ [62]. This, together with the fact that $\mathcal{G}(j, l; t)$ decay exponentially fast in time for $|j - l| \leq J_1 t$, suggests that $n_{\alpha\beta}(q, t)$ should relax in the regime $1 \ll J_1 t \ll L$. In Fig. 4 we present the mode occupation numbers $n_{\alpha\alpha}(k, t)$ at several different times for a system of size $L = 320$ prepared in the density matrix $\rho(2, 0, 0.5, 0)$ and evolved with Hamiltonian $H(0.5, 0, 0.4)$. For short and intermediate times $J_1 t < 70$ we use the full EOM, while late times are accessible only to the QBE. The QBE is initialized at time $t_0 = 20$, and is seen to be in good agreement with the full EOM until the latest times accessible by the latter method. We observe that at intermediate times both $n_{++}(k, t)$ and $n_{--}(k, t)$ slowly approach their respective thermal distributions at the effective temperature $1/\beta_{\text{eff}}$ introduced above. The “off-diagonal” occupation numbers $n_{+-}(k, t)$, calculated by integrating the full EOM, approach their thermal value zero in an oscillatory fashion. The observed behaviour of the mode occupation numbers strongly suggests that the weak integrability breaking term indeed induces thermalization.

We note that in the QBE framework the final relaxation is towards the non-interacting Fermi-Dirac distribution with an effective temperature set by the kinetic

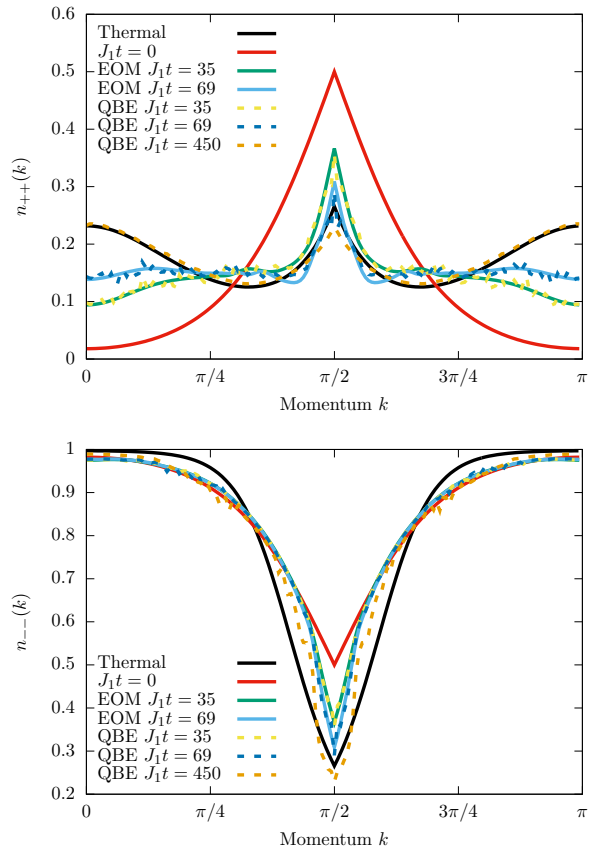


FIG. 4. (Color online) Occupation numbers $n_{++}(k, t)$ and $n_{--}(k, t)$ initialized in the thermal state (7) $\rho(2, 0, 0.5, 0)$, and time evolved with $H(0.5, 0, 0.4)$. The solid lines are the results of the EOM ($L = 320$) for various times. The dotted lines are computed by means of the QBE ($L = 320$). The black solid line is the thermal value found by means of second order perturbation theory in U .

energy at the time the Boltzmann is initialized [57, 63], signalling the importance of corrections to the QBE at very late times. Such corrections, arising from higher cumulants, are important for obtaining the power law behaviour expected at very late times (for certain observables) after quenches in non-integrable models [64, 65].

In this work we have developed a method that allows us to analyze the effects of a weak integrability breaking interaction on the time evolution of local observables after a quantum quench. We have shown that there is a crossover between a prethermalized regime, characterized by the proximity of our model to an integrable theory, and a thermal steady state. The observed drift of $\mathcal{G}(i, j; t)$ in time towards its thermal value is exponential and characterized by a time scale proportional to U^{-2} . The models considered here feature a global $U(1)$ symmetry (particle number conservation). A preliminary analysis suggests that the scenario found here, a prethermalized regime followed by a cross-over to a thermal steady state, occurs also in absence of this $U(1)$ symmetry [60].

We thank M. Fagotti, A. Gambassi, S. Kehrein and A. Silva for helpful discussions. This work was supported by the EPSRC under grants EP/J014885/1 and EP/I032487/1, by the U.S. Department of Energy, Office of Basic Energy Sciences, under Contract Nos. DEAC02-98CH10886 and DE-SC0012704 (N.J.R.) and by the Clarendon Scholarship fund (S.G.).

-
- [1] V. I. Arnold, *Mathematical Methods of Classical Mechanics*, Springer, New York, 1989.
- [2] M. Rigol, V. Dunjko, V. Yurovsky, and M. Olshanii, *Phys. Rev. Lett.* **98**, 050405 (2007).
- [3] J. M. Deutsch, *Phys. Rev. A* **43**, 2046 (1991).
- [4] M. Srednicki, *Phys. Rev. E* **50**, 888 (1994).
- [5] M. Rigol, V. Dunjko, and M. Olshanii, *Nature* **452**, 854 (2008).
- [6] M. Rigol, *Phys. Rev. Lett.* **103**, 100403 (2009).
- [7] M. Rigol and L.F. Santos, *Phys. Rev. A* **82**, 011604(R) (2010).
- [8] G. Biroli, C. Kollath, and A. M. Läuchli, *Phys. Rev. Lett.* **105**, 250401 (2010).
- [9] M. C. Bañuls, J. I. Cirac, and M. B. Hastings, *Phys. Rev. Lett.* **106**, 050405 (2011).
- [10] M. Tavora and A. Mitra, *Phys. Rev. B* **88**, 115144 (2013).
- [11] M. Rigol, *Phys. Rev. Lett.* **112**, 170601 (2014).
- [12] A. Polkovnikov, K. Sengupta, A. Silva, and M. Vengalattore, *Rev. Mod. Phys.* **83**, 863 (2011).
- [13] C. Gogolin and J. Eisert, [arXiv:1503.07538](https://arxiv.org/abs/1503.07538).
- [14] M. Rigol, A. Muramatsu, and M. Olshanii, *Phys. Rev. A* **74**, 053616 (2006).
- [15] M. A. Cazalilla, *Phys. Rev. Lett.* **97**, 156403 (2006).
- [16] P. Calabrese and J. Cardy, *J. Stat. Mech.* (2007) P06008.
- [17] M. Cramer, C. M. Dawson, J. Eisert, and T. J. Osborne, *Phys. Rev. Lett.* **100**, 030602 (2008).
- [18] T. Barthel and U. Schollwöck, *Phys. Rev. Lett.* **100**, 100601 (2008).
- [19] D. Fioretto and G. Mussardo, *New J. Phys.* **12**, 055015 (2010).
- [20] P. Calabrese, F. H. L. Essler and M. Fagotti, *Phys. Rev. Lett.* **106**, 227203 (2011); *J. Stat. Mech.* (2012) P07022.
- [21] M. Fagotti and F.H.L. Essler, *Phys. Rev. B* **87**, 245107 (2013).
- [22] J.-S. Caux and R. M. Konik, *Phys. Rev. Lett.* **109**, 175301 (2012).
- [23] F. H. L. Essler, S. Evangelisti, and M. Fagotti, *Phys. Rev. Lett.* **109**, 247206 (2012).
- [24] M. Collura, S. Sotiriadis, and P. Calabrese, *Phys. Rev. Lett.* **110**, 245301 (2013).
- [25] G. Mussardo, *Phys. Rev. Lett.* **111**, 100401 (2013).
- [26] B. Pozsgay, *J. Stat. Mech.* (2013) P07003.
- [27] M. Fagotti and F. H. L. Essler, *J. Stat. Mech.* (2013) P07012.
- [28] M. Fagotti, M. Collura, F. H. L. Essler, and P. Calabrese, *Phys. Rev. B* **89**, 125101 (2014).
- [29] B. Wouters, J. De Nardis, M. Brockmann, D. Fioretto, M. Rigol, and J.-S. Caux, *Phys. Rev. Lett.* **113**, 117202 (2014).
- [30] B. Pozsgay, M. Mestyán, M. A. Werner, M. Kormos, G. Zaránd, and G. Takács, *ibid.* **113**, 117203 (2014).
- [31] M. Kormos, M. Collura, and P. Calabrese, *Phys. Rev. A* **89**, 013609 (2014).
- [32] J. De Nardis, B. Wouters, M. Brockmann, and J.-S. Caux, *Phys. Rev. A* **89**, 033601 (2014).
- [33] S. Sotiriadis and P. Calabrese, *J. Stat. Mech.* (2014) P07024.
- [34] G. Goldstein and N. Andrei, *Phys. Rev. A* **90**, 043625 (2014).
- [35] F. H. L. Essler, G. Mussardo, and M. Panfil, *Phys. Rev. A* **91**, 051602(R).
- [36] M. Moeckel and S. Kehrein, *Phys. Rev. Lett.* **100**, 175702 (2008); *Ann. Phys.* **324**, 2146 (2009).
- [37] A. Rosch, D. Rasch, B. Binz, and M. Vojta, *Phys. Rev. Lett.* **101**, 265301 (2008).
- [38] M. Kollar, F. A. Wolf, and M. Eckstein, *Phys. Rev. B* **84**, 054304 (2011).
- [39] M. van den Worm, B.C. Sawyer, J.J. Bollinger, and M. Kastner, *New J. Phys.* **15**, 083007 (2013).
- [40] M. Marcuzzi, J. Marino, A. Gambassi, and A. Silva, *Phys. Rev. Lett.* **111**, 197203 (2013).
- [41] F. H. L. Essler, S. Kehrein, S. R. Manmana, and N. J. Robinson, *Phys. Rev. B* **89**, 165104 (2014).
- [42] N. Nessi, A. Iucci and M. A. Cazalilla, *Phys. Rev. Lett.* **113**, 210402 (2014).
- [43] M. Fagotti, *J. Stat. Mech.* (2014) P03016.
- [44] G. P. Brandino, J.-S. Caux, and R. M. Konik, [arXiv:1407.7167](https://arxiv.org/abs/1407.7167).
- [45] B. Bertini and M. Fagotti, *J. Stat. Mech.* (2015) P07012.
- [46] M. Babadi, E. Demler, and M. Knap, [arXiv:1504.05956](https://arxiv.org/abs/1504.05956).
- [47] M. Gring, M. Kuhnert, T. Langen, T. Kitagawa, B. Rauer, M. Schreitl, I. Mazets, D. Adu Smith, E. Demler, and J. Schmiedmayer, *Science* **337**, 1318 (2012).
- [48] D. Adu Smith, M. Gring, T. Langen, M. Kuhnert, B. Rauer, R. Geiger, T. Kitagawa, I. Mazets, E. Demler, and J. Schmiedmayer, *New J. Phys.* **15** 075011 (2013).
- [49] T. Langen, M. Gring, M. Kuhnert, B. Rauer, R. Geiger, D. A. Smith, I. E. Mazets, and J. Schmiedmayer, *Eur. Phys. J. Special Topics* **217**, 43 (2013).
- [50] U. Schollwöck, *Rev. Mod. Phys.* **77**, 259 (2005).
- [51] M. Stark and M. Kollar, [arXiv:1308.1610](https://arxiv.org/abs/1308.1610) (2013).
- [52] R. Orbach, *Phys. Rev.* **112**, 309 (1958).
- [53] F. H. L. Essler and R. M. Konik in *From Fields to Strings: Circumnavigating Theoretical Physics*, edited by M. Shifman, A. Vainshtein, and J. Wheeler (World Scientific, Singapore, 2005); [arXiv:0412421](https://arxiv.org/abs/0412421) (2004).
- [54] N. Nessi and A. Iucci, [arXiv:1503.02507](https://arxiv.org/abs/1503.02507) (2015).
- [55] A. Iucci and N. Nessi, *J. Phys.: Conf. Ser.* **568**, 012013 (2014).
- [56] L. Erdős, M. Salmhofer, and H.-T. Yau, *J. Stat. Phys.* **116**, 367 (2004).
- [57] J. Lukkarinen and H. Spohn, *J. Stat. Phys.* **134**, 1133 (2009).
- [58] Only states with a fixed particle number are considered in the trace.
- [59] In general the decay times for the real and imaginary parts of the Green's function are different.
- [60] B. Bertini, F. H. L. Essler, S. Groha, and N. J. Robinson, in preparation.
- [61] T.M. Wright, M. Rigol, M.J. Davis, and K.V. Kheruntsyan, *Phys. Rev. Lett.* **113**, 050601 (2014).
- [62] S. Bravyi, M. B. Hastings, and F. Verstraete, *Phys. Rev. Lett.* **97**, 050401 (2006).
- [63] M. L. R. Fürst, C. B. Mendl, and H. Spohn *Phys. Rev. E* **86**, 031122 (2012).

- [64] J. Lux, J. Müller, A. Mitra, and A. Rosch, *Phys. Rev. A* **89**, 053608 (2014).
- [65] H. Kim, M. C. Banuls, J. I. Cirac, M. B. Hastings, and D. A. Huse, *Phys. Rev. E* **92**, 012128 (2015).

Supplemental Material for ‘‘Prethermalization and thermalization in models with weak integrability breaking’’

DIAGONALIZING THE NON-INTERACTING HAMILTONIAN

The non-interacting part of the Hamiltonian (1)

$$H_0(J_2, \delta) = -J_1 \sum_l [1 + \delta(-1)^l] (c_l^\dagger c_{l+1} + c_{l+1}^\dagger c_l) - J_2 \sum_l (c_l^\dagger c_{l+2} + c_{l+2}^\dagger c_l),$$

is diagonalized by the canonical transformation

$$c_l = \frac{1}{\sqrt{L}} \sum_{k>0} \sum_{\alpha=\pm} \gamma_\alpha(l, k|\delta) a_\alpha(k), \quad (S1)$$

where the coefficients are given by

$$\gamma_\pm(2j-1, k|\delta) = e^{-ik(2j-1)}, \quad \gamma_\pm(2j, k|\delta) = \pm e^{-ik2j} e^{-i\varphi_k(\delta)}, \quad e^{-i\varphi_k(\delta)} = \frac{-\cos k + i\delta \sin k}{\sqrt{\cos^2 k + \delta^2 \sin^2 k}}.$$

In the new basis we have

$$H_0(J_2, \delta) = \sum_{\alpha=\pm} \sum_{k>0} \epsilon_\alpha(k) a_\alpha^\dagger(k) a_\alpha(k), \quad (S2)$$

where the single-particle dispersions are

$$\epsilon_\alpha(k) = -2J_2 \cos(2k) + 2\alpha J_1 \sqrt{\delta^2 + (1 - \delta^2) \cos^2(k)}. \quad (S3)$$

Applying the same transformation to the interaction part of the Hamiltonian $H_{\text{int}} = U \sum_{l=1}^L c_l^\dagger c_{l+1}^\dagger c_{l+1} c_l$ gives

$$H_{\text{int}} = U \sum_{\alpha} \sum_{\mathbf{k}>0} V_\alpha(\mathbf{k}) a_{\alpha_1}^\dagger(k_1) a_{\alpha_2}^\dagger(k_2) a_{\alpha_3}(k_3) a_{\alpha_4}(k_4). \quad (S4)$$

Here we have introduced the notations $\alpha = (\alpha_1, \alpha_2, \alpha_3, \alpha_4)$, $\mathbf{k} = (k_1, k_2, k_3, k_4)$ and $\mathbf{k} > 0$ is a shorthand notation for $k_i > 0$ for all $i = 1, \dots, 4$. The interaction vertex factor can be written in a conveniently antisymmetrized form

$$\begin{aligned} V_\alpha(\mathbf{k}) &= -\frac{1}{4} \sum_{P, Q \in S_2} \text{sgn}(P) \text{sgn}(Q) V'_{\alpha_{P_1} \alpha_{Q_1} \alpha_{P_2} \alpha_{Q_2}}(k_{P_1}, k_{Q_1}, k_{P_2}, k_{Q_2}), \\ V'_\alpha(\mathbf{k}) &= \frac{e^{i(k_3 - k_4)}}{2L} \left(\alpha_1 \alpha_2 e^{i\varphi_{k_1}(\delta)} e^{-i\varphi_{k_2}(\delta)} + \alpha_3 \alpha_4 e^{i\varphi_{k_3}(\delta)} e^{-i\varphi_{k_4}(\delta)} \right) \delta_{k_1 - k_2 + k_3 - k_4, 0} \\ &\quad + \frac{e^{i(k_3 - k_4)}}{2L} \left(\alpha_1 \alpha_2 e^{i\varphi_{k_1}(\delta)} e^{-i\varphi_{k_2}(\delta)} - \alpha_3 \alpha_4 e^{i\varphi_{k_3}(\delta)} e^{-i\varphi_{k_4}(\delta)} \right) \delta_{k_1 - k_2 + k_3 - k_4 \pm \pi, 0}, \end{aligned} \quad (S5)$$

where $P = (P_1, P_2)$ and $Q = (Q_1, Q_2)$ are permutations of (1, 2) and (3, 4) respectively.

EQUATIONS OF MOTION

The equations of motion (5) are derived by following the steps set out in Ref. [56] for deriving quantum Boltzmann equations. The starting point are the Heisenberg equations of motion (EOM) for the fermion bilinears $\hat{n}_{\alpha\beta}(q, t) = a_\alpha^\dagger(q, t) a_\beta(q, t)$. They are of the form

$$\frac{\partial}{\partial t} \hat{n}_{\alpha\beta}(k, t) = i[H, \hat{n}_{\alpha\beta}(k, t)] = i[\epsilon_\alpha(k, \delta) - \epsilon_\beta(k, \delta)] \hat{n}_{\alpha\beta}(k, t) + iU \sum_{\alpha} \sum_{\mathbf{q}>0} Y_{\alpha\beta}^\alpha(k, \mathbf{q}) \hat{A}_\alpha(\mathbf{q}, t), \quad (S6)$$

where we have defined $\hat{A}_\alpha(\mathbf{q}, t) = a_{\alpha_1}^\dagger(q_1, t) a_{\alpha_2}^\dagger(q_2, t) a_{\alpha_3}(q_3, t) a_{\alpha_4}(q_4, t)$, and

$$Y_{\alpha\beta}^\alpha(k, \mathbf{q}) = \delta_{\beta, \alpha_4} \delta_{k, q_4} V_{\alpha_1 \alpha_2 \alpha_3 \alpha}(\mathbf{q}) + \delta_{\beta, \alpha_3} \delta_{k, q_3} V_{\alpha_1 \alpha_2 \alpha \alpha_4}(\mathbf{q}) - \delta_{\alpha, \alpha_2} \delta_{k, q_2} V_{\alpha_1 \beta \alpha_3 \alpha_4}(\mathbf{q}) - \delta_{\alpha, \alpha_1} \delta_{k, q_1} V_{\beta \alpha_2 \alpha_3 \alpha_4}(\mathbf{q}).$$

In the second step we consider the Heisenberg equation of motion for the operator $\hat{A}_\alpha(\mathbf{q}, t)$

$$\frac{\partial}{\partial t} \hat{A}_\alpha(\mathbf{q}, t) = i \left[H, \hat{A}_\alpha(\mathbf{q}, t) \right] = i E_\alpha(\mathbf{q}) \hat{A}_\alpha(\mathbf{q}, t) + iU \sum_\gamma \sum_{\mathbf{p}>0} V_\gamma(\mathbf{p}) \left[\hat{A}_\gamma(\mathbf{p}, t), \hat{A}_\alpha(\mathbf{q}, t) \right], \quad (\text{S7})$$

where $E_\alpha(\mathbf{q}) \equiv \epsilon_{\alpha_1}(q_1) + \epsilon_{\alpha_2}(q_2) - \epsilon_{\alpha_3}(q_3) - \epsilon_{\alpha_4}(q_4)$. Integrating (S7) in time and then taking an expectation value with respect to our initial density matrix ρ_0 , we have

$$\langle \hat{A}_\alpha(\mathbf{q}, t) \rangle = \langle \hat{A}_\alpha(\mathbf{q}, 0) \rangle e^{itE_\alpha(\mathbf{q})} + iU \int_0^t ds \sum_\gamma \sum_{\mathbf{p}>0} e^{i(t-s)E_\alpha(\mathbf{q})} V_\gamma(\mathbf{p}) \langle [\hat{A}_\gamma(\mathbf{p}, s), \hat{A}_\alpha(\mathbf{q}, s)] \rangle.$$

Substituting this back into (S6) leads to an exact integro-differential equation for the mode occupation numbers $n_{\alpha\beta}(k, t) = \text{Tr}[\rho_0 \hat{n}_{\alpha\beta}(k, t)]$, which takes the form

$$\begin{aligned} \dot{n}_{\alpha\beta}(k, t) = & i [\epsilon_\alpha(k, \delta) - \epsilon_\beta(k, \delta)] n_{\alpha\beta}(k, t) + iU \sum_\alpha \sum_{\mathbf{q}>0} Y_{\alpha\beta}^\alpha(k, \mathbf{q}) \langle \hat{A}_\alpha(\mathbf{q}, 0) \rangle e^{itE_\alpha(\mathbf{q})} \\ & - U^2 \int_0^t ds \sum_{\alpha, \gamma} \sum_{\mathbf{q}, \mathbf{p}>0} \langle \hat{A}_\gamma(\mathbf{p}, s) \hat{A}_\alpha(\mathbf{q}, s) \rangle \left[Y_{\alpha\beta}^\alpha(k, \mathbf{q}) e^{i(t-s)E_\alpha(\mathbf{q})} V_\gamma(\mathbf{p}) - (\alpha, \mathbf{q}) \rightarrow (\gamma, \mathbf{p}) \right]. \end{aligned} \quad (\text{S8})$$

As Wick's theorem holds for all initial density matrices ρ_0 we consider, the expectation value $\langle \hat{A}_\alpha(\mathbf{q}, 0) \rangle$ can be expressed in terms of the mode occupation numbers $n_{\alpha\beta}(k, 0)$. The eight-point average in (S8) can be decomposed as

$$\langle \hat{A}_\gamma(\mathbf{p}, t) \hat{A}_\alpha(\mathbf{q}, t) \rangle = f(\{n_{\alpha\beta}(k, t)\}) + \mathcal{C}[\langle \hat{A}_\gamma(\mathbf{p}, t) \hat{A}_\alpha(\mathbf{q}, t) \rangle],$$

where the first term is the result of applying Wick's theorem, and $\mathcal{C}[\dots]$ denotes terms involving four, six and eight particle cumulants (the eight particle cumulant does not contribute because of the antisymmetric structure of (S8)). In order to turn (S8) into a closed system of integro-differential equations we now assume that the four and six particle cumulants can be neglected at all times. This leads to the following system of equations

$$\begin{aligned} \dot{n}_{\alpha\beta}(k, t) = & i\epsilon_{\alpha\beta}(k) n_{\alpha\beta}(k, t) + 4iU e^{it\epsilon_{\alpha\beta}(k)} \sum_{\gamma_1} J_{\gamma_1\alpha}(k; t) n_{\gamma_1\beta}(k, 0) - J_{\beta\gamma_1}(k; t) n_{\alpha\gamma_1}(k, 0) \\ & - U^2 \int_0^t dt' \sum_\gamma \sum_{k_1, k_2 > 0} K_{\alpha\beta}^\gamma(k_1, k_2; k; t - t') n_{\gamma_1\gamma_2}(k_1, t') n_{\gamma_3\gamma_4}(k_2, t') \\ & - U^2 \int_0^t dt' \sum_{\underline{\gamma}} \sum_{k_1, k_2, k_3 > 0} L_{\alpha\beta}^{\underline{\gamma}}(k_1, k_2, k_3; k; t - t') n_{\gamma_1\gamma_2}(k_1, t') n_{\gamma_3\gamma_4}(k_2, t') n_{\gamma_5\gamma_6}(k_3, t'), \end{aligned} \quad (\text{S9})$$

where $\underline{\gamma} = (\gamma_1, \dots, \gamma_6)$ and we introduced the functions

$$\begin{aligned} J_{\alpha\beta}(k; t) = & e^{i\epsilon_{\alpha\beta}(k)t} \sum_{\gamma_2\gamma_3} \sum_{\mathbf{q}>0} V_{\alpha\gamma_2\gamma_3\beta}(k, \mathbf{q}, \mathbf{q}, k) e^{i\epsilon_{\gamma_2\gamma_3}(\mathbf{q})t} n_{\gamma_2\gamma_3}(\mathbf{q}, 0), \\ K_{\alpha\beta}^\gamma(k_1, k_2; k; t) = & 4 \sum_{k_3, k_4 > 0} \sum_{\nu, \nu'} X_{\mathbf{k}; \mathbf{k}'}^{\gamma_1\gamma_3\nu\nu'; \nu\nu'\gamma_4\gamma_2}(\alpha, \beta; k; t), \\ L_{\alpha\beta}^{\underline{\gamma}}(k_1, k_2, k_3; k; t) = & 8 \sum_\nu \sum_{k_4 > 0} X_{\mathbf{k}; \mathbf{k}'}^{\gamma_1\gamma_3\gamma_6\nu; \nu\gamma_5\gamma_4\gamma_2}(\alpha, \beta; k; t) - 16 \sum_\nu X_{k_1 k_2 k_1 k_2; k_3 k_1 k_3 k_1}^{\gamma_1\gamma_3\nu\gamma_4; \gamma_5\nu\gamma_6\gamma_2}(\alpha, \beta; k; t), \\ X_{\mathbf{k}; \mathbf{q}}^{\gamma; \alpha}(\alpha, \beta; \mathbf{q}; t) = & Y_{\alpha\beta}^\gamma(\mathbf{k}|\mathbf{q}) V_\alpha(\mathbf{q}) e^{iE_\gamma(\mathbf{k})t} - (\gamma, \mathbf{k}) \leftrightarrow (\alpha, \mathbf{q}). \end{aligned} \quad (\text{S10})$$

The occupation numbers at time $t = 0$ for a system prepared in an initial state with density matrix $\rho(\beta, 0, \delta_i, 0)$ and time evolved with Hamiltonian $H(J_2, \delta_f, U)$ are readily calculated using Wick's theorem

$$n_{\alpha\alpha}(k) = \frac{1}{2} - \frac{1}{2} \cos(\varphi_k(\delta_f) - \varphi_k(\delta_i)) \tanh(\beta\epsilon_\alpha^{(0)}(k)/2), \quad \alpha = \pm, \quad (\text{S11})$$

$$n_{\alpha\beta}(k) = \frac{i}{2} \sin(\varphi_k(\delta_f) - \varphi_k(\delta_i)) \tanh(\beta\epsilon_\alpha^{(0)}(k)/2), \quad \alpha \neq \beta. \quad (\text{S12})$$

Here the dispersions $\epsilon_\alpha^{(0)}(k)$ are given by (S3) with $J_2 = 0$ and $\delta = \delta_i$.

QUANTUM BOLTZMANN EQUATION (QBE) FOR $\delta_f = 0$

The equations of motion obtained in our case are generally quite different from known cases, in which (matrix) QBEs can be derived [56, 57, 63]. An exception is the case $\delta_f = 0$, where it is possible to obtain a QBE for the “diagonal” occupation numbers $n_{\alpha\alpha}(q, t)$ as we will now show. Numerical integration of the full EOM, suggests that for small interactions $U \ll 1$ and at sufficiently late times $t > t_0 \sim U^{-1}$ the occupation numbers $n_{\alpha\alpha}(k, t)$ depend only on the variable $\tau \equiv U^2 t$, while $n_{+-}(k, t) \approx 0$. To describe this late time regime it is convenient take the formal scaling limit $U \rightarrow 0, t \rightarrow \infty$ keeping $\tau = tU^2$ fixed of the EOM (5). In this limit the EOM take the form

$$\begin{aligned} \dot{n}_{\alpha\alpha}(k, \tau) = & \lim_{U \rightarrow 0} 4iU^{-1} \sum_{\gamma_1} \{ J_{\gamma_1\alpha}(k; \tau U^{-2}) n_{\gamma_1\alpha}(k, 0) - J_{\alpha\gamma_1}(k; \tau U^{-2}) n_{\alpha\gamma_1}(k, 0) \} \\ & + \lim_{U \rightarrow 0} \sum_{\mathbf{k} > 0} \int_0^\tau \frac{d\sigma}{U^2} e^{iE(\mathbf{k})(\tau-\sigma)U^{-2}} F(\mathbf{k}; k; \sigma), \end{aligned} \quad (\text{S13})$$

where we have collected most of the integrand of the σ -integral into a single function $F(\mathbf{k}; k; \sigma)$ in order to lighten notations. The second contribution on the right hand side can be simplified by using our assumptions that $n_{+-}(k, \sigma) \approx 0$ and $n_{\alpha\alpha}(k, \sigma)$ are slowly varying functions of σ for $\sigma \gtrsim U$. We thus have

$$\int_0^\tau \frac{d\sigma}{U^2} e^{iE(\mathbf{k})(\tau-\sigma)U^{-2}} F(\mathbf{k}; k; \sigma) \approx \int_0^{U^{-1}} ds e^{iE(\mathbf{k})(t-s)} F(\mathbf{k}; k; s) + F(\mathbf{k}; k; \tau) \int_{U^{-1}}^t ds e^{iE(\mathbf{k})(t-s)}. \quad (\text{S14})$$

The first term vanishes in our scaling limit. We regularize the integral in the second term by replacing $E(\mathbf{k}) \rightarrow E(\mathbf{k}) + i\eta$, η is small and positive

$$\lim_{U \rightarrow 0} \int_{U^{-1}}^t ds e^{i[E(\mathbf{k})+i\eta](t-s)} = \frac{i}{E(\mathbf{k}) + i\eta} \equiv D(E(\mathbf{k})). \quad (\text{S15})$$

The first contribution on the right hand side depends only on the initial mode occupation numbers $n_{\alpha\beta}(k, 0)$. In the case $\delta_f = 0$, the leading contribution at late times is obtained by evaluating the momentum sums by a saddle point approximation. This gives

$$\frac{4i}{U} \sum_{\gamma_1} \{ J_{\gamma_1\alpha}(k; t) n_{\gamma_1\alpha}(k, 0) - J_{\alpha\gamma_1}(k; t) n_{\alpha\gamma_1}(k, 0) \} \approx \frac{\sin(\epsilon_{+-}(0)t)}{Ut^{3/2}} (A_\alpha(k) e^{i\epsilon_{+-}(k)t} + \text{c.c.}), \quad (\text{S16})$$

where $A_\alpha(k)$ is an amplitude depending on the initial state and the vertex function. The right hand side of (S16) vanishes in the scaling limit. Putting everything together, we obtain the following QBE in the scaling limit

$$\begin{aligned} \dot{n}_{\alpha\alpha}(k, \tau) = & - \sum_{\gamma} \sum_{k_1, k_2 > 0} \tilde{K}_{\alpha\alpha}^{\gamma_1\gamma_2}(k_1, k_2; k) n_{\gamma_1\gamma_1}(k_1, \tau) n_{\gamma_2\gamma_2}(k_2, \tau) \\ & - \sum_{\gamma} \sum_{k_1, k_2, k_3 > 0} \tilde{L}_{\alpha\alpha}^{\gamma_1\gamma_2\gamma_3}(k_1, k_2, k_3; k) n_{\gamma_1\gamma_1}(k_1, \tau) n_{\gamma_2\gamma_2}(k_2, \tau) n_{\gamma_3\gamma_3}(k_3, \tau). \end{aligned} \quad (\text{S17})$$

Here the kernels are given by

$$\begin{aligned} \tilde{K}_{\alpha\beta}^{\gamma_1\gamma_2}(k_1, k_2|q) &= 4 \sum_{k_3, k_4 > 0} \sum_{\nu, \nu'} \tilde{X}_{\mathbf{k}|\mathbf{k}'}^{\gamma_1\gamma_2\nu\nu'} | \nu\nu'\gamma_2\gamma_1(\alpha, \beta|q), \\ \tilde{L}_{\alpha\beta}^{\gamma_1\gamma_2\gamma_3}(k_1, k_2, k_3|q) &= 8 \sum_{\nu} \sum_{k_4 > 0} \tilde{X}_{\mathbf{k}|\mathbf{k}'}^{\gamma_1\gamma_2\gamma_3\nu} | \nu\gamma_3\gamma_2\gamma_1(\alpha, \beta|q) - 16 \sum_{\nu} \tilde{X}_{k_1 k_2 k_1 k_2 | k_3 k_1 k_3 k_1}^{\gamma_1\gamma_2\nu\gamma_2}(\alpha, \beta|q), \\ \tilde{X}_{\mathbf{k}|q}^{\gamma}(\alpha, \beta|q) &= Y_{\alpha\beta}^{\gamma}(\mathbf{k}|q) V_{\alpha}(\mathbf{q}) D(E_{\gamma}(\mathbf{k})) - (\gamma, \mathbf{k}) \leftrightarrow (\alpha, \mathbf{q}). \end{aligned} \quad (\text{S18})$$

When implementing the QBE for finite L , the parameter η in (S15) must be kept finite (see e.g. [63]). The results presented in this paper are for $\eta = 0.0005$.